Synthesis, Biodistribution, and Primate Imaging of Fluorine-18 Labeled 2β-Carbo-1′-fluoro-2-propoxy-3β-(4-chlorophenyl)tropanes. Ligands for the Imaging of Dopamine Transporters by Positron Emission Tomography

Dongxia Xing,[†,‡] Ping Chen,[†,‡] Robert Keil,[†,‡] Clinton D. Kilts,[†,§] Bing Shi,[†,‡] Vernon M. Camp,[†,‡] Gene Malveaux,[†,‡] Timothy Ely,[§] Michael J. Owens,[§] John Votaw,[†,‡] Margaret Davis,[†,∥] John M. Hoffman,[†,‡] Roy A. E. BaKay,[⊥] Thygarajan Subramanian,[∥] Ray L. Watts,[∥] and Mark M. Goodman*[,†,‡]

Emory Center for Positron Emission Tomography and Departments of Radiology, Psychiatry and Behavior Sciences, Neurology, and Neurosurgery, Emory University, Atlanta, Georgia 30320

Received May 5, 1999

2β-(*R*)-Carbo-1-fluoro-2-propoxy-3β-(4-chlorophenyl)tropane ((*R*)-FIPCT, *R*-**6**) and 2β-(*S*)-carbo-1-fluoro-2-propoxy-3β-(4-chlorophenyl)tropane ((*S*)-FIPCT, *S*-**6**) were prepared and evaluated in vitro and in vivo for dopamine transporter (DAT) selectivity and specificity. High specific activity [^{18}F](*R*)-FIPCT and [^{18}F](*S*)-FIPCT were synthesized in 5% radiochemical yield (decay-corrected to end of bombardment (EOB)) by preparation of the precursors 2β-carbo-*R*-1-mesyloxy-2-propoxy-3β-(4-chlorophenyl)tropane (*R*-**12**) and 2β-carbo-*S*-1-mesyloxy-2-propoxy-3β-(4-chlorophenyl)tropane (*S*-**12**) followed by treatment with no carrier-added potassium[^{18}F]-fluoride and kyrptofix K222 in acetonitrile. Competition binding in cells stably expressing the transfected human DAT and serotonin transporter (SERT) labeled by [^{3}H]WIN 35428 and [^{3}H]-citalopram, respectively, demonstrated the following order of DAT affinity (K_i in nM): GBR 12909 (0.36) > CIT (0.48) > (*S*)-FIPCT (0.67) ≫ (*R*)-FIPCT (3.2). The affinity of (*S*)-FIPCT and (*R*)-FIPCT for SERT was 127- and 20-fold lower, respectively, than for DAT. In vivo biodistribution studies were performed in male rats and demonstrated that the brain uptake of [^{18}F](*R*)-FIPCT and [^{18}F](*S*)-FIPCT were selective and specific for DAT rich regions (caudate and putamen). PET brain imaging studies in monkeys demonstrated high [^{18}F](*R*)-FIPCT and [^{18}F](*S*)-FIPCT uptake in the caudate and putamen which resulted in caudate-to-cerebellum and putamen-to-cerebellum ratios of 2.5−3.5 at 115 min. [^{18}F](*R*)-FIPCT uptake in the caudate/putamen achieved transient equilibrium at 75 min. In an imaging experiment with [^{18}F](*S*)-FIPCT in a rhesus monkey with its left hemisphere lesioned with MPTP, radioactivity was reduced to background in the caudate and putamen of the lesioned hemisphere. The high specific activity one-step radiolabeling preparation and high specificity and selectivity of [^{18}F](*R*)-FIPCT and [^{18}F](*S*)-FIPCT for DAT indicate [^{18}F](*R*)-FIPCT and [^{18}F](*S*)-FIPCT are potential radioligands for mapping brain DAT in humans using PET.

Introduction

The dopamine transporter (DAT) complex is a protein that is located on the membranes of presynaptic mesotelencephalic dopaminergic neurons which originate in the substantia nigra and ventral tegmentum located in the midbrain and converge to the basal ganglia of the forebrain. The DAT, a member of the family of Na^+ Cl^--dependent transporters, mediates uptake of dopamine (DA) by an electrogenic sodium and chloride transport coupled mechanism. Alterations of the density and function of DAT have been implicated in psychomotor disorders such as Parkinson's disease,[1−3] Huntington's chorea,[3] and schizophrenia.[4] It is also widely accepted that the reinforcing, psychomotor stimulant, and euphoric effects of cocaine are initiated by the drug-induced inhibition of DAT associated with mesolimbocortical DA systems.[5−9] These findings have resulted in the development of a number of positron emitting radioligands[10−16] for quantitating cerebral DAT density using positron emission tomography (PET). The most extensively investigated series of carbon-11 and fluorine-18 labeled radioligands for imaging the density of DAT are those in which the 3β-(benzoyl) group of (−)-cocaine was replaced by 3β-(4-substituted-phenyl) groups.[17] Several analogues of this series of 2β-carbomethoxy-3β-(4-substituted-phenyl)tropanes were found to be greater than 100 times more potent than (−)-cocaine.

The radiolabeling methods utilized for the preparation of the carbon-11 tropanes involved either N-alkylation of the 8-position of the corresponding nortropane or O-alkylation of *N*-fluoroalkyl nortropane 2β-carboxylic acids with high specific activity $^{11}CH_3I$. The carbon-11 labeled DAT imaging agents include [^{11}C]2β-carbomethoxy-3β-(4-fluorophenyl)tropane ([^{11}C]-WIN 35,428/CFT),[18−21] [^{11}C]2β-carbomethoxy-3β-(4-iodophenyl)tropane ([^{11}C]CIT/RTI-55),[22] [^{11}C]2β-carbomethoxy-3β-(4-

* Address correspondence and requests for reprints to Mark M. Goodman, Ph.D., Emory University, Dept. of Radiology, 1364 Clifton Road, NE, Atlanta, GA 30322. Phone: (404) 727-9366. Fax: (404) 727-3488. E-mail: mgoodma@emory.edu.
† Emory Center for Positron Emission Tomography.
‡ Department of Radiology.
§ Department of Psychiatry and Behavior Sciences.
∥ Department of Neurology.
⊥ Department of Neurosurgery.

10.1021/jm9902234 CCC: $19.00
Published on Web 01/29/2000

chlorophenyl)tropane ([^{11}C]CCT),[21] [^{11}C]2β-carbomethoxy-3β-(3,4-dichlorophenyl)tropane ([^{11}C]CDCT),[21] [^{11}C]3β-(4-iodophenyl)tropane-2β-carboxylic acid isopropyl ester ([^{11}C]RTI-121),[23] *N*-3-fluoropropyl-2β-carbomethoxy-3β-(4-iodophenyl)nortropane (*O*-methyl-[^{11}C]FP-CIT) [24] and *N*-2-fluoroethyl-2β-carbomethoxy-3β-(4-iodophenyl)nortropane ([^{11}C] β-CIT-FE).[25] An undesired property accompanying DAT binding by [^{11}C]-WIN 35,428, [^{11}C]-CCT, [^{11}C]CDCT, and [^{11}C]CIT/RTI-55 in nonhuman and human primates is the need for a prolonged (>2 h) period required to reach binding equilibrium with the DAT. Unlike the parent, [^{11}C]CIT/RTI-55, *O*-methyl-[^{11}C]FP-CIT, and [^{11}C]β-CIT-FE DAT binding have been reported to reach a transient equilibrium.[24,25]

Fluorine-18 offers an advantage in comparison to the short 20 min half-life of carbon-11 for ligands which show delayed binding equilibrium. Fluorine-18's 110 min half-life allows a longer time (3 × 110 min) for imaging radioligands which require a longer period of time to reach a binding equilibrium. Radiosyntheses of fluorine-18 labeled *N*-3-fluoropropyl-2β-carbomethoxy-3β-(4-iodophenyl)nortropane (β-CIT-FP),[26] 2β-carbo-2′-fluoroethoxy-3β-(4-chlorophenyl)tropane (FECT),[27] 2β-carbo-2′-fluoroethoxy-3β-(4-methylphenyl)tropane (FETT),[27] 2β-carbomethoxy-3β-(4-chlorophenyl)-8-(3-fluoropropyl)nortropane (FPCT),[28] and 2β-carbomethoxy-3β-(4-chlorophenyl)-8-(2-fluoroethyl)nortropane (FECNT)[29] in which the methyl group at the 8-position of the tropane was replaced by a 3-fluoropropyl group and a 2-fluoroethyl group and the 2β-methyl ester by a 2β-2′-fluoroethyl ester have recently been reported. Fluorine-18 labeled FPCT and FECNT were prepared by a two-step reaction sequence which first involved the preparation of the radiolabeled precursors 1-[^{18}F]fluoro-3-iodopropane and 1-[^{18}F]fluoro-2-tosyloxyethane, respectively, followed by alkylation with 2β-carbomethoxy-3β-(4-chlorophenyl)nortropane to afford [^{18}F]FPCT and [^{18}F]FECNT in 15−21% overall yield corrected for decay at EOB. In a similar manner, fluorine-18 labeled FECT and FETT were prepared from the radiolabeled precursor 1-[^{18}F]fluoro-2-bromopropane followed by alkylation with 2β-carboxy-3β-(4-chlorophenyl)tropane and 2β-carboxy-3β-(4-methylphenyl)tropane.[27] A successful one-step radiosynthesis of fluorine-18 labeled FP-CIT has been reported,[26] though in only a 1% radiochemical yield. The necessity to employ a two-step reaction sequence to achieve good reproducible radiochemical yields is a major shortcoming for the use of the *N*-[^{18}F]-fluoroalkylnortropanes and *O*-[^{18}F]fluoroalkyltropanes for potential widespread clinical use. Fluorine-18 labeled DAT ligands prepared in high specific activity and good radiochemical yield by a one-step radiolabeling method are more desirable for production and distribution in a hospital based radiopharmacy.

In addition to high affinity and specificity, high selectivity is another important characteristic for a DAT radioligand developed for in vivo imaging. Recently, it was reported that replacement of the 2β-carbomethoxy functionality of 3β-(*p*-substituted-phenyl)-*N*-methyl-tropane-2β-carboxylic acid methyl esters with an isopropyl ester affords analogues exhibiting a significant enhancement in selectivity for the dopamine transporter in comparison to norepinephrine (NET) and serotonin (SERT) transporters.[29] The 4-chloro derivative (CTC-

Scheme 1[a]

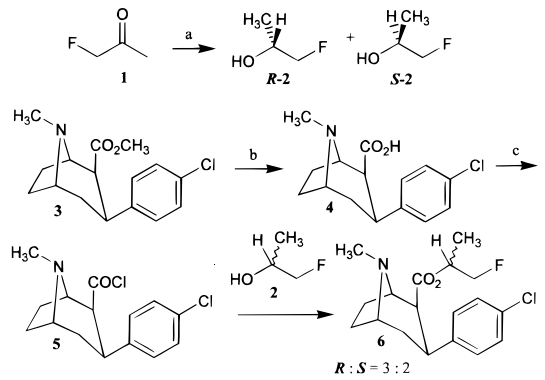

[a] Reagents: (a) $LiAlH_4$, diethyl ether; (b) 1:1 dioxane: H_2O; (c) $POCl_3$.

^{i}Pr) was found to show low nanomolar potency (IC_{50} = 1.41 nM vs [^{3}H]CFT) and to be 1000 times more selective for the DAT than the SERT (IC_{50} = 1404 nM using [^{3}H]paroxetine) and NET (IC_{50} = 2154 nM vs [^{3}H]-mazindol). These results suggested that the replacement of the 2β-carbomethoxy functionality of CTC-^{i}Pr with a 2β-(*R,S*) 2′-fluoroisopropoxy bioisostere may also lead to a high affinity and highly selective ligand for the DAT.

In this paper we report the synthesis of 2β-(*R,S*)-carbo-1′-fluoro-2-propoxy-3β-(4-chlorophenyl)tropane ((*R,S*)-FIPCT), the diastereomeric syntheses of 2β-(*R*)-carbo-1′-fluoro-2-propoxy-3β-(4-chlorophenyl)tropane ((*R*)-FIPCT) and 2-β-(*S*)-carbo-1′-fluoro-2-propoxy-3β-(4-chlorophenyl)tropane ((*S*)-FIPCT), in vitro and in vivo evaluation, and a one-step radiochemical synthesis and PET imaging in nonhuman primates to evaluate the effect of the 2β-(*R*)-1′-fluoro-2-propoxy and 2β-(*S*)-1′-fluoro-2-propoxy substituents on striatal affinity, uptake, and retention of the two new tropane analogues *R*-FIPCT and *S*-FIPCT. These new analogues are attractive candidates for labeling with fluorine-18 for quantitating cerebral DAT density using positron emission tomography (PET).

Chemistry

The 2β-(*R,S*)-carbo-1′-fluoro-2-propoxy-3β-(4-chlorophenyl)tropane (*R,S*-FIPCT) (**6**) DAT ligand of this study was prepared in a four step sequence of reactions delineated in Scheme 1. In this synthetic approach, fluoroacetone (**1**) was treated with $LiAlH_4$ to form an enantiomeric mixture of (*R,S*)-1-fluoro-2-propanol (**2**). 2β-Carboxy-3β-(*p*-chlorophenyl)tropane (**4**) was prepared from 2β-carbomethoxy-3β-(*p*-chlorophenyl)tropane (**3**) by treatment with a 1:1 mixture of dioxane and H_2O under gentle reflux.[29] 2β-Carboxy-3β-(*p*-chlorophenyl)tropane (**4**) was converted to 2β-methanoyl chloride-3β-(*p*-chlorophenyl)tropane (**5**)[29] by treatment with phosphorus oxychloride. Esterification of acid chloride **5** with (*R,S*)-1-fluoro-2-propanol (**2**) gave *R,S*-FIPCT (**6**) as a 3:2 *R*:*S* mixture of diastereomers as determined by high-pressure liquid chromatographic analysis (HPLC).

The synthetic approach chosen for the preparation of diastereomerically pure 2β-(*R*)-carbo-1′-fluoro-2-propoxy-3β-(4-chlorophenyl)tropane ((*R*)-FIPCT) (*R*-**6**) and 2β-(*S*)-carbo-1′-fluoro-2-propoxy-3β-(4-chlorophenyl)tropane ((*S*)-FIPCT) (*S*-**6**) involved the use of the commer-

Scheme 2[a]

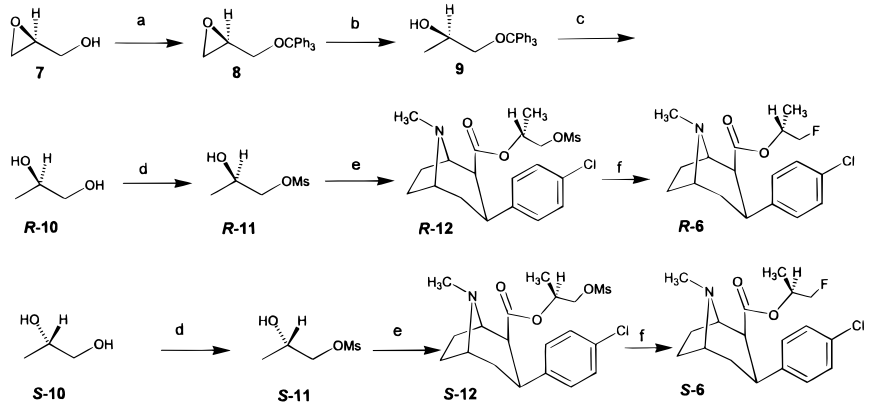

[a] Reagents: (a) Ph_3CCl, pyridine; (b) $LiAlH_4$, THF; (c) Pd/C, H_2, MeOH; (d) MsCl, NEt_3, CH_2Cl_2; (e) **5**, NEt_3, CH_2Cl_2; (f) $N(C_4H_9)_4F$, THF.

cially available optically active C-3 synthons (*S*)-glycidol (**7**) and (*S*)-1,2-propandiol (*S*-**10**), respectively. The use of these chiral materials facilitated the construction of either the *R*- or *S*- diastereochemical configurations of **6** to enable a study of the structure−activity relationships on DAT binding for the (*R*)-FIPCT and (*S*)-FIPCT diastereomers. In this synthetic approach, 2β-carbo-*R*-1′-mesyloxy-2-propoxy-3β-(4-chlorophenyl)tropane (*R*-**12**) and 2β-carbo-*S*-1′-mesyloxy-2-propoxy-3β-(4-chlorophenyl)tropane (*S*-**12**) were the key substrates employed for selectively introducing fluorine onto the 1′-position of the corresponding 2β-carbo-*R*-1′-fluoro-2-propoxy (*R*-**6**) and 2β-carbo-*S*-1′-fluoro-2-propoxy (*S*-**6**) esters. The key substrate *R*-**12** was prepared from a six-step sequence of reactions outlined in Scheme 2. (*S*)-Glycidol (**7**) was treated with triphenylmethyl chloride to give (*S*)-1-triphenylmethylglicydyl ether (**8**). Reduction of the aryloxyglycidyl **8** with lithium aluminum hydride afforded (*R*)-1-triphenylmethoxy-2-propanol (**9**). Hydrogenolysis of **9** by treatment with Pd/C and H_2 gave (*R*)-1,2-propandiol (*R*-**10**) in quantitative yield. Treatment of the diol *R*-**10** with methanesulfonyl chloride gave (*R*)-1-mesyloxy-2-propandiol (*R*-**11**) which was converted to 2β-carbo-(*R*-1′-mesyloxy-2-propoxy)-3β-(4-chlorophenyl)-tropane (*R*-**12**) by esterification of acid chloride **5**. The 2β-carbo-*S*-1′-mesyloxy-2-propoxy-3β-(4-chlorophenyl)-tropane (*S*-**12**) substrate was prepared in an analogous manner in two steps from (*S*)-1,2-propandiol (*S*-**10**) (Scheme 2).

The pivotal step in the syntheses of 2β-(*R*)-carbo-1′-fluoro-2-propoxy-3β-(4-chlorophenyl)tropane ((*R*)-FIPCT) (*R*-**6**) and 2β-(*S*)-carbo-1′-fluoro-2-propoxy-3β-(4-chlorophenyl)tropane ((*S*)-FIPCT) (*S*-**6**) involved introduction of fluoride into the 2β-carbo-2-propoxy group by treatment with tetrabutylammonium fluoride. The 2β-(*R*)-carbo-1′-fluoro-2-propoxy esters *R*-**6** and *S*-**6** were purified by flash chromatography followed by crystallization. HPLC analysis (C_{18}) of *R*-**6** and *S*-**6** showed the presence of only one diastereomer.

Radiochemistry

Fluorine-18 labeled *R,S*-FIPCT ([^{18}F]**6**) was prepared, shown in Scheme 3, by treatment of the corresponding mesylate with potassium[^{18}F]fluoride and kryptofix K222 in acetonitrile at 100 °C to give a mixture of *R,S*-FIPCT ([^{18}F]**6**) and the 2α-epimer in a 4:6 ratio as

Scheme 3

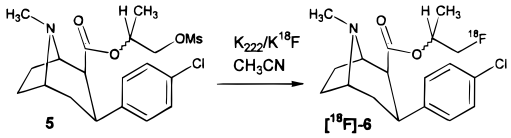

determined by HPLC analysis using a radioactivity detector. Semipreparative, reverse-phase HPLC purification of the epimeric mixture gave *R,S*-FIPCT (**6**) in 4.6% radiochemical yield, corrected for decay at end of bombardment (EOB), in a synthesis time of 100 min following bombardment and with a specific activity of 2 Ci/μmol as determined from the mass measured from the HPLC UV analysis. The diastereomerically pure fluorine-18 labeled *R*-FIPCT ([^{18}F]*R*-**6**) and *S*-FIPCT ([^{18}F]*S*-**6**) were prepared in an analogous manner from their corresponding mesylates.

A shortcoming of the radiosynthesis of fluorine-18 *R,S*-FIPCT is the significant conversion to its 2α-epimer. Radiochemical yields of the desired fluorine-18 2β-epimer ranged from 1.4 to 4.6% at the end of synthesis and were accompanied by an additional 2.7 to 6.5% of the undesired 2α-epimer. If the conversion of the 2β- to the 2α-epimer could be minimized, then the end of synthesis radiochemical yield of fluorine-18 *R,S*-FIPCT may be increased to 7%. It is feasible that the *R,S*-FIPCT 2α-epimer resulted from either epimerization, by K222/K_2CO_3, of the 2β-mesylate precursor prior to radiofluorination or epimerization of the final radiolabeled product. We investigated the preparation of fluorine-18 labeled *R,S*-FIPCT by reducing the quantity of K222/K_2CO_3. We ran triplicate experiments in which 0.5 equiv of K222/K_2CO_3 was used. The reduced K222/K_2CO_3 preparations produced *R,S*-FIPCT in 4.9% (n = 3) radiochemical yield at end of bombardment and resulted in less conversion, 0.17% (n = 3), of the 2α-epimer.

Biological Results

The in vitro affinities of *R*-FIPCT and *S*-FIPCT for the DAT were determined by competition in DAT radioligand binding assays using [^{3}H]-WIN 35,428 binding in homogenates of murine kidney cells stably expressing the human DAT and are shown in Table 1. The rank order of affinities was GBR 12909 > CIT > *S*-FIPCT > CCT-^{i}Pr > *R*-FIPCT. *R*-FIPCT had 6 times

Table 1. Inhibition Constants (K_i, nM) of Various Ligands for Monoamine Transporters

	human			rat			
ligand	DA[a]	5-HT[b]	5-HT/DA ratio	DA[c]	5-HT[c]	NE[c]	5-HT/DA ratio
CIT	0.48	0.67	1.4				
CCT-^{i}Pr	0.9	427	474				
R-FIPCT	3.2	64	20	14.7	133	498	9
S-FIPCT	0.67	85	127	6.06	137	690	23
GBR 12909	0.36						
fluvoxamine		3.08					

[a] Competitive binding versus [*N*-methyl-^{3}H]-WIN 35,428 in murine kidney cells transfected with human dopamine transporter. [b] Competitive binding versus [^{3}H]citalopram in murine kidney cells transfected with human serotonin transporter. [c] Samples (2−12 nM) of [*N*-methyl-^{3}H]-WIN 35,428, [^{3}H]citalopram, or [^{3}H]desmethylipramine were incubated in the presence of 7−11 concentrations of the indicated ligand and membranes prepared from rat striatum or cortex. The assays were performed by NOVASCREEN in participation with the NIMH/NOVASCREEN Psychotherapeutic Drug Discovery Development Program.

lower affinity than CIT, for the human transfected DAT. In comparison to *S*-FIPCT and CCT-^{i}Pr, *R*-FIPCT had 4 and 3 times, respectively, lower affinity for the transfected human DAT. Similarly, in comparison to *S*-FIPCT, *R*-FIPCT had 2.5 times lower affinity for DAT binding in rat striatal homogenates. Competition binding site analyses were also used to evaluate the comparative affinity of *R*-FIPCT and *S*-FIPCT for the human SERT and NET labeled by [^{3}H]citalopram and [^{3}H]desmethylipramine, respectively (Table 1). The affinity of *R*-FIPCT and *S*-FIPCT for the human SERT was 20- and 127-fold lower, respectively, than for DAT. A lower selectivity for *R*-FIPCT and *S*-FIPCT for the DAT vs the SERT, 9 and 23 respectively, was noted in binding studies using rat cortical homogenates (Table 1). These results indicate that *R*-FIPCT and *S*-FIPCT exhibit low affinity for the rat NET and selective affinity for human and rat DAT vs SERT and that *S*-FIPCT exhibited both higher affinity and selectivity for the human and rat DAT than *R*-FIPCT.

The diastereomeric mixture and the *R*- and *S*-isomers of FIPCT were labeled with fluorine-18, and the distribution of radioactivity expressed as percent dose per gram in tissues of male rats is shown in Table 2. The accumulation of radioactivity in the bone was initially low and exhibited no increase from 2 min (0.13% dose/g) to 2 h (0.1% dose/g), which demonstrated the expected stability of the fluoroisopropyl group to significant in vivo defluorination.

The individual *R*- and *S*-diastereomers of FIPCT were labeled with flourine-18, and the regional distribution study in the brain of male Sprague Dawley rats was performed over 2 h. The results shown in Tables 3 and 4 demonstrate that [^{18}F]-*R*-**6** (Table 3) showed high initial striatal uptake and moderate retention. The striatum uptake reached a maximum at 30 min (4.50% dose/g). After 120 min, the striatum uptake decreased 73% when compared to the peak activity at 30 min. The S/Cereb and S/CX ratios reached a maximum 6.0 and 3.0, respectively, at 60 min. The high uptake of fluorine-18 in regions of the brain expressing DATs and high S/Cereb ratio at 60 min and the 73% washout in the striatum over 120 min demonstrate that [^{18}F]-*R*-**6** has potential favorable kinetic properties for in vivo quantitation and imaging of the DAT by PET.

Table 2. Distribution of Radioactivity (Percent Injected Dose per Gram of Tissue) in Rats after iv Administration of *R*,*S*-[^{18}F]FIPCT[a]

	time after injection			
tissue	2 min	30 min	60 min	120 min[b]
blood	0.06 (10.05−0.07)	0.01 (0.01−0.01)	0.01 (0.01−0.01)	0.01 (0.01−0.01)
heart	0.76 (0.64−0.93)	0.06 (0.05−0.07)	0.05 (0.04−0.05)	0.06 (0.04−0.08)
lungs	2.57 (2.0−3.75)	0.35 (0.29−0.38)	0.18 (0.15−0.21)	0.23 (0.18−0.34)
liver	0.74 (0.69−0.82)	2.06 (1.82−2.37)	2.23 (2.13−2.42)	2.09 (1.64−2.45)
spleen	0.74 (0.68−0.85)	0.22 (0.2−0.26)	0.14 (0.14−0.15)	0.14 (0.1−0.18)
kidneys	1.49 (1.13−1.94)	0.18 (0.17−0.18)	0.11 (0.1−0.11)	0.12 (0.09−0.16)
muscle	0.05 (0.04−0.05)	0.05 (0.04−0.06)[b]	0.04 (0.02−0.05)	0.04 (0.03−0.05)
testis	0.07 (0.06−0.07)	0.09 (0.07−0.1)	0.09 (0.07−0.1)	0.08 (0.08−0.09)
bone	0.13 (0.1−0.15)	0.08 (0.07−0.08)	0.07 (0.06−0.07)	0.1 (0.01−0.13)

[a] Mean and range (in parentheses) values for four male Sprague−Dawley rats. [b] Mean and range (in parentheses) values for three male Sprague−Dawley rats.

Table 3. Distribution of Radioactivity (Percent Injected Dose per Gram of Tissue) in Rat Brain Regions after iv Administration of *R*-[^{18}F]FIPCT[a]

	time after injection			
region	5 min	30 min	60 min	120 min
striatum	3.97 (3.44−4.80)	4.50 (3.57−6.08)	2.28 (2.07−2.83)	1.20 (1.07−1.22)
cortex (CX)	2.76 (2.47−3.09)	2.04 (1.67−2.66)	0.77 (0.51−1.09)	0.40 (0.22−0.33)
cerebellum	1.42 (1.26−1.62)	0.99 (0.75−1.23)	0.38 (0.32−0.48)	0.22 (0.19−0.25)
rest of brain	1.36 (1.19−1.53)	1.03 (0.85−1.21)	0.45 (0.36−0.52)	0.27 (0.22−0.33)
S/Cereb	2.79 (2.49−3.81)	4.55 (3.83−4.94)	6.0 (4.43−6.93)	5.45 (4.64−6.14)
S/CX	1.44 (1.32−1.94)	2.21 (1.67−2.85)	2.96 (2.59−4.06)	3.0 (2.61−3.24)

[a] Mean and range (in parentheses) values for four male Sprague−Dawley rats.

Table 4. Distribution of Radioactivity (Percent Injected Dose per Gram of Tissue) in Rat Brain Regions after iv Administration of *S*-[^{18}F]FIPCT[a]

	time after injection			
region	5 min	30 min[b]	60 min[b]	120 min
striatum	2.47 (1.89−3.73)	2.82 (2.7−3.03)	2.6 (2.13−2.89)	1.78 (1.19−3.39)
cortex (CX)	1.16 (0.92−1.36)	1.07 (0.92−1.19)	0.45 (0.36−0.51)	0.29 (0.21−0.39)
cerebellum	0.77 (0.68−0.89)	0.59 (0.52−0.73)	0.22 (0.17−0.27)	0.14 (0.12−0.17)
rest of brain	0.83 (0.63−0.98)	0.69 (0.62−0.80)	0.33 (0.24−0.39)	0.21 (0.16−0.25)
S/Cereb	3.21 (2.12−4.65)	4.78 (4.2−5.29)	11.82 (10.37−12.54)	12.7 (8.04−20.19)
S/CX	2.13 (1.70−2.74)	2.64 (2.31−2.93)	5.78 (4.19−5.82)	6.14 (4.25−8.69)

[a] Mean and range (in parentheses) values for four male Sprague−Dawley rats. [b] Mean and range (in parentheses) values for three male Sprague−Dawley rats.

The *S*-diastereomer of FIPCT, [^{18}F]-*S*-**6** (Table 4), showed higher striatal retention and S/Cereb and S/CX ratios in comparison to the *R*-diastereomer. In addition, in contrast with [^{18}F]-*R*-**6**, the [^{18}F]-*S*-**6** striatum uptake

Figure 1. Trans-axial image for a single plane following 5.69 mCi of [^{18}F](*S*)-FIPCT (*S*-**6**) summed for 105−125 min in a male rhesus monkey.

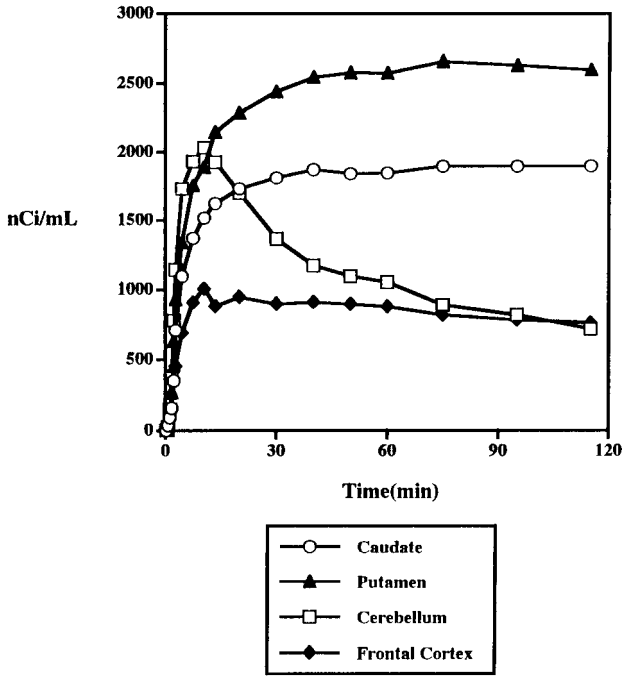

Figure 2. Time−activity curves for brain regions for a rhesus monkey after receiving 3.33 mCi of [^{18}F](*R*)-FIPCT (*R*-**6**). Serial images were acquired for a total time of 125 min (i.e., 18 scans).

decreased only 37% when compared to the peak activity at 30 min. The S/Cereb and S/CX ratios of [^{18}F]-*S*-**6** exhibited a pronounced increase with time. The S/Cereb and S/CX ratios at 120 min were 12.7 and 6.14, respectively. The higher striatal uptake and retention of the *S*-diastereomer in comparison to the *R*-diastereomer are consistent with the results of the in vitro competitive binding data which show that the *S*-diastereomer exhibits a 2.5- to 5-fold higher affinity for the DAT. These results indicate that [^{18}F]-*S*-**6** may also have very good potential for imaging the DAT in the striatum and extrastriatal sites by PET.

In Vivo Nonhuman Primate Imaging

PET imaging studies were performed with [^{18}F]-*R*-**6** and [^{18}F]-*S*-**6** to compare and determine time−activity curves for brain regions-of-interest in rhesus monkeys at 0−115 min post injection. The distribution of fluorine-18 in the brain following administration of [^{18}F]-*R*-**6** and [^{18}F]-*S*-**6** was characteristic of binding to DAT sites. The highest uptake occurred in the caudate and putamen, with the lowest uptake occurring in the cerebellum and cortex. (Figure 1).

Time-activity curves of the caudate and putamen exhibiting the kinetics of the two diastereomers [^{18}F]-*R*-**6** and [^{18}F]-*S*-**6** in the monkeys (Figure 2 and Figure 3) were consistent with the results found in the rats. The studies performed in rats demonstrated that [^{18}F]-*R*-**6** cleared more rapidly than [^{18}F]-*S*-**6** from the striatum. In the PET imaging study with [^{18}F]-*R*-**6** in the rhesus monkey, the putamen and caudate achieved a transient equilibrium at 75 min post injection, whereas the decay-corrected uptake of [^{18}F]-*S*-**6** continued to increase at 115 min post injection. Following administration of [^{18}F]-*R*-**6**, the putamen exhibited the highest uptake in the brain of the monkey and attained maximum (0.08% dose/g) uptake at 75 min. The uptake percentage of [^{18}F]-*R*-**6** in the cerebellum (CB) and cortex (CX) exhibited a maximum value of 0.06% dose/g at 10. 5 min and 0.03% dose/g at 4.5 min post injection, respectively. The putamen-to-cerebellum and putamen-to-cortex exhibited ratios ranged from 3.4 to 3.6 at 115 min. Caudate radioactivity indicated a peak uptake of 0.06% dose/g at 75 min and a caudate-to-cerebellum and caudate-to-cortex ratio of 2.5−2.6 at 115 min. The [^{18}F]-*S*-**6** diastereomer, which showed prolonged retention in the striatum, exhibited 0.06% dose/g and 0.05% dose/g in putamen and caudate, respectively, at 115 min. The putamen-to-cerebellum and caudate-to-cerebellum ratios were 2.5−2.6 at 115 min.

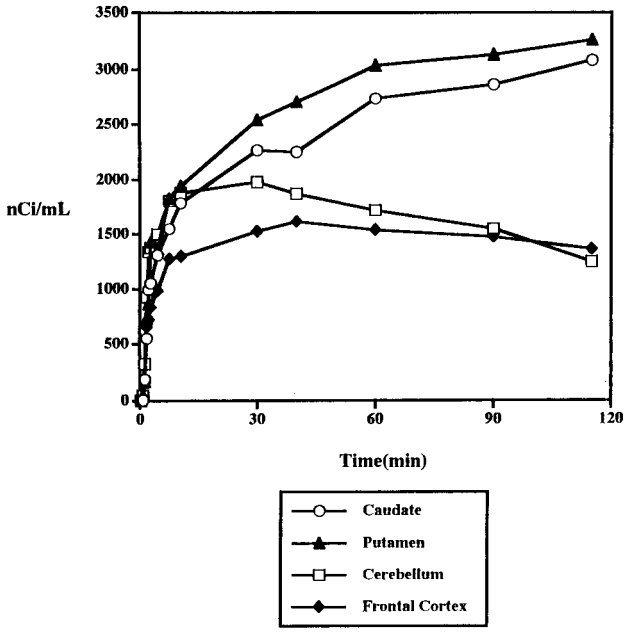

Figure 3. Time−activity curves for brain regions for a rhesus monkey after receiving 5.69 mCi of [^{18}F](*S*)-FIPCT (*S*-**6**). Serial images were acquired for a total time of 125 min (i.e., 18 scans).

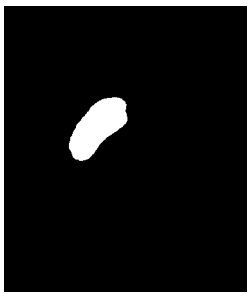

Figure 4. Trans-axial image for a single plane following 2.95 mCi of [^{18}F](*S*)-FIPCT (*R*-**6**) summed for 105−125 min in a male rhesus monkey previously given a left intracarotid infusion of MPTP.

The in vivo binding of [^{18}F]-*S*-**6** to the DAT in the caudate and putamen of a rhesus monkey was demonstrated further by the absence of striatal radioactivity in the left hemisphere of a monkey which previously received a left intracarotid infusion of MPTP. The uptake of radioactivity in the caudate and putamen was only present in the right hemisphere of the rhesus monkey brain at 115 min following injection of [^{18}F]-*S*-**6**. The putamen-to-cerebellum and caudate-to-cerebellum ratios in the right hemisphere were 3.4−3.5 at 115 min while the putamen-to-cerebellum and caudate-to-cerebellum ratios in the left hemisphere were 1.2−1.4 at 115 min.

Metabolite Analysis

Arterial plasma samples from a rhesus monkey following femoral vein injection of *S*-[^{18}F]FIPCT and *R*-[^{18}F]FIPCT were analyzed for nonpolar, potentially brain permeable metabolites by a solvent extraction and TLC method. The major radioactive component appearing in the initial arterial plasma samples was ether extractable, displayed a single peak (>98% pure) on TLC, and corresponded to unmetabolized authentic *S*-[^{18}F]FIPCT. The fraction of plasma radioactivity corresponding to unmetabolized *S*-[^{18}F]FIPCT rapidly decreased from 86% at 5 min to 30% at 30 min. The major radiolabeled metabolite found in arterial plasma was a polar nonextractable component, which increased to 89% of the plasma activity by 120 min. The identity of the polar metabolite was not elucidated due to its improbable brain permeability. The metabolite profile for *R*-[^{18}F]FIPCT demonstrated that this diastereomer metabolized more rapidly. The fraction of plasma radioactivity corresponding to unmetabolized *R*-[^{18}F]-FIPCT rapidly decreased from 84% at 3 min to 25% at 14 min. The major radiolabeled metabolite found in arterial plasma was a polar nonextractable component, which increased to 95% of the plasma activity by 120 min. Thus, there was no detectable formation of lipophilic radiolabeled metabolites from either diastereomer that was capable of entering the brain. The absence of labeled lipophilic metabolites in the arterial plasma that could reenter the brain permits the metabolism uncorrected calculation of the *S*-[^{18}F]FIPCT and *R*-[^{18}F]FIPCT input function and subsequent quantification of binding sites by tracer kinetic modeling.

Conclusions

The two diastereomers of FIPCT (**6**) have been synthesized and radiolabeled with fluorine-18 by a one-step method in a synthesis time of 85 min including HPLC purification. Competition binding assays in cells stably expressing the human monoamine transporters demonstrated that *S*-**6** and *R*-**6** have a high affinity for the DAT with *S*-**6** showing the highest selectivity, 127-fold higher for the DAT over the SERT. Biodistribution studies in rats showed that both [^{18}F]-*S*-**6** and [^{18}F]-*R*-**6** exhibited high uptake in the striatum, a region rich in DAT sites. PET imaging studies in rhesus monkeys demonstrated that [^{18}F]-*R*-**6** achieved a transient equilibrium in the striatum in less than 90 min and is an attractive candidate for in vivo quantitation of DAT sites by PET. In contrast, [^{18}F]-*S*-**6** exhibited potential for mapping extrastriatal DAT sites due to prolonged retention within the striatum after 115 min which will afford higher signal-to-background ratios than [^{18}F]-*R*-**6** after 115 min.

Experimental Section

All chemicals and solvents were analytical grade and were used without purification. The fluorine-18 fluoride was obtained from 95% enriched oxygen-18 water (Enritiech) by proton irradiation with a Seimens RDS 112, 11 MeV cyclotron. The melting points (mp) were determined in capillary tubes using an Electrothermal apparatus and are uncorrected. The thin-layer chromatographic analyses (TLC) were performed using 250 μm thick layers of silica gel G PF-254 coated on aluminum plates (Whatman). The proton nuclear magnetic resonance (NMR) spectra were obtained at 300 or 400 MHz with a Varian instrument. Carbon-13 nuclear magnetic resonance spectra were obtained at 300 or 400 MHz with a Varian instrument. Elemental analyses were performed by Atlantic Microlab, Inc. (Norcross, GA) and, unless noted otherwise, were within ±0.4% of the calculated values. High-resolution voltage scans were performed at 70 EV with reference scans over narrow mass, •0.0006. Analyses were within 0.002 of theoretical values. Mass spectra (MS) were determined on a ZAB-EQ (VG Analytical) hybrid high-resolution, double-focusing mass spectrometer with collision and analyzing quadropole.

All animal experiments were carried out according to protocols approved by the Institutional University Animal Care Committee (IUCAC) and Radiation Safety Committees of Emory University.

Chemistry. (*R,S*)-1-Fluoro-2-propanol (2). A solution of fluoroacetone (1.0 g, 13 mmol) in anhydrous ethyl ether (5 mL) was added dropwise to a stirred suspension of $LiAlH_4$ (131 mg, 3.25 mmol) in 15 mL of anhydrous ethyl ether at −70 °C over a period of 1 min. The reaction mixture was allowed to warm to room temperature. The resulting mixture was stirred at 40 °C for 10 min, then cooled to room temperature, and acidified to pH 3 with 10% H_2SO_4 solution. The aqueous phase was separated and extracted with ether (4 × 15 mL). The combined organic phase was washed with saturated $NaHCO_3$ and brine, dried over anhydrous $MgSO_4$, and concentrated in vacuo to give **2** (460 mg, 46%) as a colorless liquid, bp 105 °C. The product was used without further purification: ^{1}H NMR ($CDCl_3$) δ 1.18 (dd, J = 1.5, 3.6 Hz, 3 H), 3.45 (s, 1 H), 3.98−4.12 (m,1H), 4.24 (ddd, J = 6.9, 9.3, 48 Hz, 1 H), 4.35 (ddd, J = 3.0, 9.3, 47 Hz, 1 H).

***N*-Methyl-3β(4-chlorophenyl)tropane-2β-carboxylic Acid (4).** A solution of **3** (200 mg, 0.68 mmol) in H_2O/dioxane (1:1, 8 mL) was refluxed for 3 days. After the reaction, the solvents were removed and the residue was purified via flash column chromatography (eluted employing a gradient with 20% MeOH in CH_2Cl_2 (0.1% Et_3N) to 50% MeOH in CH_2Cl_2 (0.1% Et_3N)) to afford **4** as a colorless microcrystalline solid (180 mg, 95%): ^{1}H NMR (D_2O) δ 1.75−1.85 (m, 1 H), 1.95−2.13 (m, 2 H), 2.20−2.40 (m, 2 H), 2.56−2.78 (m, 2 H), 2.69 (s, 3 H), 3.27−3.40 (1 H), 3.82−3.95 (m, 2 H), 7.16 (*AB*, J = 8.4 Hz, 1 H), 7.26 (*AB*, J = 8.4 Hz, 1 H).

***N*-Methyl 2β-carbo-(*R,S*)-1-fluoro-2-isopropanoxy-3β-(4-chlorophenyl)tropane (*R,S*-6).** A suspension of **4** (115 mg, 0.41 mmol) in $POCl_3$ (0.8 mL) was stirred under argon at room temperature for 4 h. Then excess $POCl_3$ was removed under reduced pressure. Toluene (3 mL) was added and then removed under reduced pressure to dryness. The freshly prepared *R,S*-**2** (190 mg, 1.23 mmol) in anhydrous CH_2Cl_2 (2.5 mL) was added, followed by Et_3N (0.2 mL) under argon at 0 °C. The resulting mixture was stirred at 10 °C overnight. H_2O (10 mL) was added, the resulting solution was basified with NH_4OH, extracted with CH_2Cl_2 (4 × 10 mL), dried ($MgSO_4$), and filtered, and the filtrate was concentrated in vacuo. The resulting oil was purified via flash column chromatography (eluted gradually from Et_2O to 1% Et_3N in Et_2O) to afford *R*-**12** as a colorless microcrystalline solid (141 mg, 83%): mp 109−110 °C; ^{1}H NMR ($CDCl_3$) δ 1.12 (d, J = 6.6 Hz, 3 H), 1.55−1.76 (m, 4 H), 2.02−2.28 (m, 1 H), 2.19 (s, 3 H), 2.51 (dt, J =

2.7, 12.3 Hz, 1 H), 2.83 (s, 3 H), 2.86−3.02 (m, 2 H), 3.32−3.40 (m, 1 H), 3.54−3.60 (m, 1 H), 4.00−4.15 (m, 2 H), 4.98−5.10 (m, 1 H), 7.16−7.28 (m, 4 H).

(*S*)-1-Triphenylmethyl Glycidyl Ether (8). A solution of (*S*)-glycidol (**7**, 5 g, 64.8 mmol) in pyridine (16 mL) was cooled to 0 °C under argon. Then triphenylmethyl chloride (18.06 g, 64.8 mmol) was added. The resulting mixture was allowed to warm to room temperature and stirred overnight. The resulting mixture was washed with saturated aqueous $CuSO_4$ solution, extracted with EtOAc, dried ($MgSO_4$), and filtered. The filtrate was concentrated in vacuo to give an oil that was purified via flash column chromatography (1% EtOAc in hexane) to afford a colorless microcrystal solid (**8**, 6.5 g, 32%): ^{1}H NMR ($CDCl_3$) δ 2.65−2.70 (m, 1 H), 2.79−2.85 (m, 1 H), 3.15−3.25 (m, 2 H), 3.35−3.40 (m, 1 H), 7.25−7.58 (m, 15 H).

(*R*)-1-Triphenylmethoxy-2-propanol (9). A solution of **8** (3 g, 9.48 mmol) in anhydrous THF (12 mL) was cooled to 0 °C under argon. $LiAlH_4$ (190 mg, 19 mmol, 95%) was added, and the resulting mixture was stirred continuously overnight. The reaction was quenched with H_2O, followed by 6 N NaOH. The suspension was filtered, the filtrate was extracted with CH_2Cl_2 (4 × 30 mL), dried ($MgSO_4$), and filtered, and the filtrate was concentrated in vacuo. The resulting oil was purified via flash column chromatography (1% EtOAc in hexane) to afford a colorless microcrystalline solid (**8**, 1.93 g, 64%): ^{1}H NMR ($CDCl_3$) δ 0.98 (d, J = 6.3 Hz, 3 H), 2.362 (d, J = 3 Hz, 1 H for OH), 2.93 (dd, J = 16.8, 9.0 Hz, 1 H), 3.02 (dd, J = 9.3, 3.4 Hz, 1 H), 3.80 (m, 1 H), 7.10−7.45 (m, 15 H).

(*R*)-1,2-Propanediol (*R*-10). To a solution of **9** (3.58 g, 21.5 mmol) in methanol (25 mL) was added Pd/C (800 mg) and H_2. The resulting mixture was stirred at room temperature overnight. The resulting suspension was filtered, and the residue was washed with CH_2Cl_2 (2 × 2 mL). The combined filtrates were concentrated in vacuo, and the product (*R*-**10**) was distilled out under reduced pressure via Kujelrohr to afford a clear oil (1.64 g, 100%): ^{1}H NMR ($CDCl_3$) δ 1.04 (d, J = 6.6 Hz, 3 H), 3.28 (dd, J = 19.2, 11.2 Hz, 1 H), 3.48 (dd, J = 2.7 Hz, 1 H), 3.72−3.85 (m, 1 H), 4.44 (s, 2 H for OHs).

(*R*)-2-Hydroxy-propyl Methanesulfate (*R*-11). A solution of *R*-**10** (180 mg, 2.37 mmol) in anhydrous CH_2Cl_2 (2 mL) and Et_3N (0.24 mL) was cooled to 0 °C under argon, and then methanesulfonyl chloride (271 mg, 2.37 mmol) was added dropwise. After the addition, the resulting mixture was allowed to warm to room temperature over a period of 2 h. Ice water (5 mL) was added, the product was extracted with CH_2Cl_2 (4 × 10 mL), dried ($MgSO_4$), and filtered, and the filtrate was concentrated in vacuo. The resulting oil was purified via flash column chromatography (5% Et_2O in CH_2Cl_2, 0.03% Et_3N) to afford *R*-**11** as a colorless oil (230 mg, 57%): ^{1}H NMR ($CDCl_3$) δ 1.11 (d, J = 6.0 Hz, 3 H), 2.96 (s, 3 H), 3.92−4.12 (m, 3 H).

(*S*)-2-Hydroxy-propyl Methanesulfate (*S*-11). A solution of *S*-**10** (180 mg, 2.37 mmol) in anhydrous CH_2Cl_2 (2 mL) and Et_3N (0.24 mL) was cooled to 0 °C under argon and then allowed to react with methanesulfonyl chloride (271 mg, 2.37 mmol) as described for *R*-**11**. The resulting oil was purified via flash column chromatography (5% Et_2O in CH_2Cl_2, 0.03% Et_3N) to afford *S*-**11** as a colorless oil (230 mg, 57%): ^{1}H NMR ($CDCl_3$) δ 1.11 (d, J = 6.0 Hz, 3 H), 2.96 (s, 3 H), 3.92−4.12 (m, 3 H).

***N*-Methyl-2β-carbo-(*R*)-1′-mesyl-2-propoxy-3β-(4-chlorophenyl)tropane (*R*-12).** A suspension of **4** (115 mg, 0.41 mmol) in $POCl_3$ (0.8 mL) was stirred at room temperature for 4 h. The $POCl_3$ was removed under reduced pressure. Toluene (3 mL) was added and then removed under reduced pressure to dryness. The freshly prepared *R*-**11** (190 mg, 1.23 mmol) in anhydrous CH_2Cl_2 (2.5 mL) was added, followed by Et_3N (0.2 mL) under argon at 0 °C. The resulting mixture stirred at 10 °C overnight. H_2O (10 mL) was added, the resulting solution was basified with NH_4OH, extracted with CH_2Cl_2 (4 × 10 mL), dried ($MgSO_4$), and filtered, and the filtrate was concentrated in vacuo. The resulting oil was purified via flash column chromatography (eluted gradually from Et_2O to 1% Et_3N in Et_2O) to afford *R*-**12** as a colorless microcrystalline solid (141 mg, 83%): mp 109−110 °C; ^{1}H NMR ($CDCl_3$) δ 1.12 (d J = 6.6 Hz, 3 H), 1.55−1.76 (m, 4 H), 2.02−2.28 (m, 1 H), 2.19 (s, 3 H), 2.51 (dt, J = 2.7, 12.3 Hz, 1 H), 2.83 (s, 3 H), 2.86−3.02 (m, 2 H), 3.32−3.40 (m, 1 H), 3.54−3.60 (m, 1 H), 4.00−4.15 (m, 2 H), 4.98−5.10 (m, 1 H), 7.16−7.28 (m, 4 H); HRMS (EI) Calcd for $C_{19}H_{26}ClNO_5S$: 415.1220. Found: 415.1228.

***N*-Methyl-2β-carbo-(*R*)-1′-fluoro-2-propoxy-3β-(4-chlorophenyl)tropane (*R*-6).** To a solution of *R*-**12** (18 mg, 0.043 mmol) in 1:1 Et_2O/THF (2 mL) was added a solution of 1 M $Bu_4N^+F^-$ in THF (0.05 mL) under argon. The resulting mixture was refluxed for 7 h. After the reaction, the solvents were removed, and the residue was purified via flash column chromatography (eluted gradually from Et_2O to 0.5% Et_3N in Et_2O) to afford *R*-**6** as a colorless microcrystalline solid (8 mg, 56%): mp 98−99 °C; ^{1}H NMR ($CDCl_3$) δ 1.08 (dd, J = 0.9, 6.6 Hz, 3 H), 1.48−1.75 (m, 4 H), 2.00−2.25 (m, 1 H), 2.16 (s, 3 H), 2.41 (dt, J = 3.0, 12.3 Hz, 1 H), 2.75−2.90 (m, 2 H), 3.25−3.40 (m, 1 H), 3.50−3.60 (m, 1 H), 4.10 (d, J = 3.9 Hz, 1 H), 4.26 (d, J = 3.6 Hz, 1 H), 4.80−5.00 (m, 1 H), 7.14−7.25 (m, 4 H); HRMS (EI) Calcd for $C_{18}H_{23}ClFNO_2$: 339.1401. Found: 339.1406.

***N*-Methyl-2β-carbo-(*S*)-1′-mesyl-2-propoxy-3β-(4-chlorophenyl)tropane (*S*-12).** A suspension of **4** (100 mg, 0.357 mmol) in $POCl_3$ (0.8 mL) were allowed to react as described for the preparation of *R*-**12**. The resulting acid chloride **5** and mesylate *S*-**11** (180 mg, 1.17 mmol) in anhydrous CH_2Cl_2 (2.5 mL) were reacted and worked up as described above for the preparation of *R*-**12**. The resulting oil was purified via flash column chromatography (eluted gradually from Et_2O to 1% Et_3N in Et_2O) to afford *S*-**12** as a colorless microcrystalline solid (124 mg, 84%): mp 91.0−91.5 °C; ^{1}H NMR ($CDCl_3$) δ 1.04 (d, J = 6.6 Hz, 3 H), 1.47−1.72 (m, 4 H), 1.96−2.20 (m, 1 H), 2.15 (s, 3 H), 2.44 (dt, J = 2.6, 12.5 Hz, 1 H), 2.78−2.98 (m, 2 H), 2.94 (s, 3 H), 3.24−3.34 (m, 1 H), 3.50−3.56 (m, 1 H), 4.00 (dd, J = 10.8, 5.4 Hz, 1 H), 4.10 (dd, J = 10.8, 3.6 Hz, 1 H), 4.90−5.00 (m, 1 H), 7.07−7.22 (m, 4 H); ^{13}C NMR ($CDCl_3$) d 16.04 (q), 25.13 (t), 25.83 (t), 33.12 (t), 33.86 (d), 37.61 (q), 41.78 (d), 52.51 (q), 62.10 (d), 65.05 (d), 66.77 (d), 70.59 (t), 128.0 (d), 128.6 (d), 131.5 (s), 141.5 (s), 170.5 (s); HRMS (EI) Calcd for $C_{19}H_{26}ClNO_5S$: 415.1220. Found: 415.1228.

***N*-Methyl-2β-carbo-(*S*)-1′-fluoro-2-propoxy-3β-(4-chlorophenyl)tropane (*S*-6).** To a solution of *S*-**12** (120 mg, 0.29 mmol) in THF (5 mL) was added a solution of 1 M $Bu_4N^+F^-$ in THF (0.33 mL) under argon. The resulting mixture was refluxed for 7 h. After the reaction, the solvent was removed and the residue was purified via flash column chromatography (eluted gradually from Et_2O to 0.5% Et_3N in Et_2O) to afford *S*-**6** as a colorless microcrystalline solid (32 mg, 33%): mp 102.5−103.5 °C; ^{1}H NMR ($CDCl_3$) δ 1.03 (dd, J = 0.9, 6.6 Hz, 3 H), 1.48−1.70 (m, 4 H), 1.95−2.25 (m, 1 H), 2.14 (s, 3 H), 2.48 (dt, J = 3.0, 12.5 Hz, 1 H), 2.80−2.95 (m, 2 H), 3.26−3.32 (m, 1 H), 3.50−3.57 (m, 1 H), 4.06−4.38 (m, 2 H), 4.81−5.00 (m, 1 H), 7.10−7.20 (m, 4 H); ^{13}C NMR ($CDCl_3$) d 15.05 (q, d, J = 7.0 Hz), 25.18 (t), 25.71 (t), 33.16 (t), 33.85 (d), 41.73 (d), 52.53 (q), 62.10 (d), 65.23 (d), 67.96 (d, d, J = 19.9 Hz), 84.44 (t, d, J = 172.6 Hz), 127.9 (d), 128.5 (d), 131.4 (s), 141.6 (s), 170.6 (s); Anal. Calcd for $C_{18}H_{23}ClFNO_2$: C, 63.62; H, 6.82; N, 4.12. Found: C, 63.55; H, 6.83; N, 4.09.

FIPCT Radiolabeling. Approximately 280 μL of 95% enriched [^{18}O]water containing 430 mCi NCA [^{18}F]fluoride (Seimens RDS 112) was added to an 11 mL glass reaction vessel containing 1 mL of a solution of 5 mg of Kryptofix (K-222) and 0.5 mg of potassium carbonate in 0.05 mL of water and 0.95 mL of CH_3CN. The solution was heated at 118 °C for 3.5 min after which three additional portions of 1 mL of CH_3CN were added and evaporated to dry the fluoride. The vial was cooled to room temperature, and 3 mg of 2β-carbo-(*R*,*S*-1′-mesyloxy-2-propoxy)-3β-(4-chlorophenyl)tropane (*R*,*S*-**12**) dissolved in 1.0 mL of CH_3CN was added. The solution was heated to 100 °C for 10 min, cooled to room temperature, diluted with 4 mL of ether, and passed through a Waters classic SiO_2 sep-pak into a 10 mL maxi-vial attached to a 50 mL round-bottomed flask. The sep-pak was rinsed with 4 mL

of Et_2O, which was added to the maxi-vial, bringing the total volume to 10 mL. The resulting ethereal solution was evaporated by gentle heating and with a stream of argon gas. The resulting residue was dissolved in 1 mL of 80/10/0.1% methanol/water/triethylamine and injected onto a reverse-phase prep high-pressure liquid chromatography (HPLC) column (Waters, 25 mm × 100 mm, flow rate 6 mL/min). The fraction eluting at 14 min contained 0.18 mCi (0.07%, end of bombardment (EOB)) of fluorine-18 labeled 2α-carbo-(*R,S*-1′-fluoro-2-propoxy)-3*β*-(4-chlorophenyl)tropane. The fraction eluting at 19 min contained 15.19 mCi (6%, EOB) of the desired product *R,S*-FIPCT ([^{18}F]**6**), in a synthesis/purification time of 85 min. Thin-layer chromatography (TLC) analysis of *R,S*-FIPCT ([^{18}F]-**6**) using a radioactivity detector (SiO_2, 90:10 CH_2Cl_2:CH_3OH, $R_f = 0.42$) and HPLC analysis (Waters C_{18}, 8 mm × 200 mm Novapak, 75/25/0.1% methanol/water/triethylamine, flow rate 1 mL/min, rt = 5.38 min) using a UV detector and a radioactivity detector showed these fractions to have a radiochemical purity of greater than 99%. Fractions containing the greatest radioactivity were concentrated in vacuo, dissolved in sterile saline with 10% ethanol, and filtered through an Acrodisc 0.2 μm filter for in vivo studies.

Animal Tissue Distribution Experiments. The distribution of radioactivity was determined in tissues of male Sprague−Dawley rats (225−300 g) after intravenous administration of the radioiodinated tropane. The animals were allowed food and water ad libitum prior to the course of the experiment. The radiofluorinated tropanes [^{18}F]*R,S*-**6**, [^{18}F]*S*-**6**, and [^{18}F]*R*-**6** (50 μCi) in 0.2 mL of 13% EtOH in 0.9% NaCl were injected directly into the tail vein of rats under ketamine anesthesia. The animals were sacrificed at various time points post injection by cardiac excision under ketamine anesthesia, and the organs were excised, rinsed, and blotted dry. The organs were weighed, and the radioactivity of the contents was determined with a Packard γ automatic counter (Model Cobra). The percent dose per organ was calculated by a comparison of the tissue counts to suitably diluted aliquots of injected material. Total activities of blood and muscle were calculated under the assumption that they were 7% and 40% of the total body weight, respectively.

Regional brain distribution was obtained in male Sprague−Dawley rats (225−300 g) after intravenous administration of [^{18}F]*R,S*-**6**, [^{18}F]*S*-**6**, and [^{18}F]*R*-**6**. The cortex, striatum, and cerebellum were dissected and placed in tared test tubes. The test tubes were weighed, and the radioactivity of the contents was determined with a γ automatic counter. The percent dose per gram was calculated by a comparison of the tissue counts with the counts of the diluted initial injected dose. The uptake ratio of each brain region was obtained by dividing the percent/gram of each region by that of the cerebellum.

Tissue Preparation. Male Sprague−Dawley rats (200−250 g) were decapitated under ether anesthesia, and the brains were excised and placed in ice. Striatal tissues were dissected, pooled, and homogenized in 100 volumes (w/v) of ice cold Tris-HCl buffer (50 mM, pH 7.4). The striatal homogenates were centrifuged at 20000*g* for 20 min, and the resultant pellets were rehomogenized in the same buffer and recentrifuged. The final pellets were resuspended in a buffer composed of 50 mM Tris buffer, pH 7.4; 120 mM NaCl; 5 mM KCl; 2 mM $CaCl_2$; and 1 mM $MgCl_2$ and kept at −20° C for the binding assay detailed below.

Binding Assays. Tissue preparations (50 μL, 40−60 μg protein) were incubated with appropriate amounts of [^{3}H] labeled ligand and competitors in a total volume of 0.2 mL of the assay buffer. The assay mixture was incubated for 60 min at room temperature with stirring, and the resulting samples were rapidly filtered through Whatman GF/B glass-fiber filters pretreated with 0.2% protamine base and washed with 3 × 5 mL of cold (4° C) 50 mM Tris-HCl buffer, pH 7.4. The nonspecific binding was obtained in the presence of 10 mM (−)-cocaine. The filters were counted in a γ counter (Beckman 5500) at an efficiency of 70%. Saturation binding, Scatchard, and competition experiments were analyzed with the iterative nonlinear least squares curve-fitting program.

In Vitro Binding Experiments. Monoamine transporter binding assays used cell membranes from either a dog kidney (MDCK) cell line stably transfected with the human DAT cDNA (gift of Dr. Gary Rudnick, Yale University) or a human embryonic kidney cell line (HEK-293) stably transfected with the human serotonin (hSERTcDNA (gift of Randy Blakely, Ph.D., Vanderbilt University). Cells were grown to confluency in DMEM containing 10% fetal bovine serum and Geneticin sulfate and were harvested using 37° C phosphate-buffered saline (PBS, pH 7.4) containing ethylenediaminetetracetic acid (EDTA). Following centrifugation (2000*g*, 10 min), the supernatants were decanted and the pellets homogenized with a Polytron PT3000 (Brinkman, Littau, Switzerland, 11 000 rpm for 12 s) in 30 volumes of PBS and centrifuged at 43 000*g* for 10 min. The supernatants were decanted and the resulting pellets stored at −70° C until assayed.

Binding assays were carried out in 12 × 75 mm polystyrene tubes in a 1000 μL volume consisting of 700 μL of assay buffer, 100 μL of competing ligand, 100 μL of [^{3}H] ligand, and 100 μL of membrane suspension. Prior to each assay, the cell lines were characterized to determine a membrane concentration that yielded optimal binding. Membrane suspensions were prepared by resuspending the pellet in 5 mL of assay buffer and centrifuging (400*g*, 10 min). The supernatant was decanted, and the resulting pellet resuspended in assay buffer and briefly homogenized using a Polytron PT3000. Competing ligands were assayed in triplicate at each of nine concentrations (10^{-13} to 10^{-6} M). The ligands were first dissolved in absolute ethanol at 10^{-3} M then serially diluted in 2.5 mM HCl. A monoamine transporter-selective ligand of known binding affinity (DAT, GBR 12909; hSERT, fluvoxamine) was included as a reference in each assay. For DAT binding, the assay buffer was 0.03 M phosphate buffer (pH 7.4) containing 0.32 M sucrose, the radioligand was [^{3}H]-WIN 35,428 (Dupont NEN, Boston, MA, 84.5 Ci/mmol, 2.0 nM final concentration), and the equilibrium incubation time was 2 h at 4° C. For hSERT binding, the assay buffer was 50 mM Tris, 120 mM NaCl, 5 mM KCl (pH 7.9), the radioligand was [^{3}H]citalopram (Dupont NEN, Boston, MA, 85.7 Ci/mmol, 0.5 nM final concentration), and the equilibrium incubation time was 1 h at 22° C. All assays were initiated by the addition of membrane suspension. Incubations were terminated by the addition of 2 mL of 0.03 M phosphate buffer (pH 7.4, 4° C) and rapid vacuum filtration through GF/B filters (presoaked in phosphate buffer containing 0.3% polyethyleneimine) with four washes (5 mL) of 0.03 M phosphate buffer (pH 7.4, 4° C). The filters were then dried and placed in scintillation vials to which 6 mL of scintillation cocktail (Aquasol-2, Packard, Meriden, CT) was added. The vials were shaken and radioactivity was determined in a liquid scintillation counter at 66% efficiency. The data from the competition binding curves were analyzed and K_i values generated using GraphPad Prism software (GraphPad Software, San Diego, CA).

Nonhuman Primate Imaging. Quantitative brain images were acquired in a male rhesus monkey weighing 12.1 kg and a female rhesus monkey weighing 5 kg using a Seimens 951 31 slice PET imaging system. Images were reconstructed with a Shepp-Logan filter (0.35 × Nyquist frequency) giving a resolution of 8 mm fwhm. The animal was anesthetized, initially, with Telazol (3 mg/kg; i.m.) and maintained on a 1% isofluorane/5% oxygen mixture throughout the imaging procedure. The animals were intubated with assurance of adequate patency of the airway and were placed on a ventilator with arterial blood gases monitored throughout the study to ensure physiologic levels of respiration. An arterial catheter was placed in a distal leg artery of the animals. The animals were placed in the tomograph, and the head was immobilized with a thermoplastic (Tru Scan, MD) face mask. A transmission scan was then obtained with a gallium source for attenuation correction of emission data. [^{18}F]FIPCT samples, 5.69 mCi and 3.13 mCi, were injected into an antecubital vein of the male and female, respectively, in a slow bolus infusion over 30 s. Arterial blood sampling (0.5 mL samples) was performed at approximately 10−12 s intervals with 12 samples

obtained over the first 2 min. Arterial samples were also obtained at 3, 4, 5, 7, 10, 20, 30, 60, 90, and 120 min after tracer injection. Kinetic emission data were acquired either using an 18 frame acquisition sequence which included six 30 s scans, four 3 min scans, five 10 min scans, and three 20 min scans or using a 20 frame acquisition sequence which included six 30 s scans, four 3 min scans, five 10 min scans, three 20 min scans, and two 30 min scans. Bilateral regions of interest on the [^{18}F]FIPCT images were drawn manually for the caudate, putamen, frontal cortex, and cerebellum. The data were displayed as both % dose/g and nCi/mL and normalized for the quantity of injected dose and the weight of the monkey. A left intracarotid infusion of MPTP was performed on the female rhesus monkey by a previously reported method,[30] several weeks prior to the PET study.

[^{18}F]FIPCT Metabolite Analysis (Monkey). Arterial plasma analysis of *S*-[^{18}F]FIPCT metabolism was performed in a rhesus monkey. Metabolite analysis was performed as described for [^{18}F]FPCT.[28] [^{18}F]FIPCT was injected as described above, and arterial samples (5.0 mL) were collected at approximately 2, 5, 15, 30, 60, and 120 min after tracer injection. Plasma was prepared by centrifugation (3000*g* for 20 min), and nonpolar, brain permeable ^{18}F labeled metabolites were extracted with ethyl ether (2 × l mL). The ethyl ether extracts of each plasma sample were evaporated to dryness under nitrogen at 35 °C. The resulting residue was dissolved in 200 μL of 90:10 CH_2Cl_2:CH_3OH and analyzed by TLC (SiO_2) with a radioactivity detector.

Acknowledgment. This research was sponsored by the Office of Health and Environmental Research, U.S. Department of Energy, under Grant No. DE-FG05-93ER61737 and the National Institute of Mental Health Drug Screening Program. The authors thank Carolyn K. Malcolm for assistance in preparing the manuscript, Delicia Votaw, and Teresa Abak for assistance in the data collection and analysis.

References

(1) Niznik, H. B.; Fogel, E. F.; Fassos, E. F.; Seeman P. The Dopamine Transporter is Absent in Parkinson's Putamen and Reduced in the Caudate Nucleus. *J. Neurochem*. **1991**, *56*, 192−198.

(2) Kaufman, M. J.; Madras, B. K. Severe Depletion of Cocaine Recognition Sites Associated with the Dopamine Transporter in Parkinson's Diseased Striatum. *Synapse* **1991**, *49*, 43−49.

(3) Bernheimer, H.; Birkmayer, W.; Hornykiewcz, O. Brain Dopamine and the Syndromes of Parkinson and Huntington: Clinical, Morphological and Neurochemical Correlations. *J. Neurol. Sci*. **1973**, *20*, 415−455.

(4) Haberland, N.; Hetey, L. J. Studies in Postmortem Dopamine Uptake. II. Synaptosomal Catecholamine Uptake in Postmortem Brain Regions in Schizophrenia. *J. Neural. Transm*. **1987**, *68*, 303−13.

(5) Reith, M. E. A.; Meisler, B. E.; Sershen, H.; Lajtha, A. Structural Requirements For Cocaine Congeners to Interact with Dopamine and Serotonin Uptake Sites in Mouse Brain and To Induce Stereotyped Behavior. *Biochem. Pharmacol*. **1986**, *35*, 1123−1129.

(6) Giros, B.; Jaber, M.; Jones, S. R.; Wightman, R. M.; Caron, M. G. Hyper-locomotion and Indifference to Cocaine and Amphetamine in Mice Lacking the Dopamine Transporter. *Nature* **1996**, *379*, 606−612.

(7) Ritz, M. C.; Lamb, R. J.; Goldberg, S. R.; Kuhar, M. J. Cocaine Receptors on Dopamine Transporters are Related to Self-administration of Cocaine. *Science* **1987**, *237*, 1219−1223.

(8) Volkow, N. D.; Wang, G. J.; Fischman, M. W.; Foltin, R. W.; Fowler, J. S.; Abumrad, N. N.; Vitkun, S.; Logan, J.; Gatley, S. J.; Pappas, N.; Hitzemann, R.; Shea, C. E. Relationship Between Subjective Effects of Cocaine and Dopamine Transporter Occupancy. *Nature* **1997**, *386*, 827−830.

(9) Volkow, N. D.; Wang, G. J.; Fowler, J. S.; Logan, J.; Gatley, S. J.; Hitzemann, R.; Chen, A. D.; Dewey, S. L.; Pappas, N. Decreased Striatal Dopaminergic Responsiveness in Detoxified Cocaine-dependent Subjects. *Nature* **1997**, *386*, 830−833.

(10) Aquilonius, S. M.; Bergstrom, K.; Eckernas, S. A.; Hartvig, P.; Leendeers, K. L.; Lundquist, H.; Antoni, G.; Gee, A.; Rimland, A.; Uhlin, J.; Langstrom, B. In Vivo Evaluation of Striatal Dopamine Reuptake Sites Using ^{11}C-Nomifensine And Positron Emission Tomography. *Acta Neurol. Scand*. **1987**, *76*, 283−287.

(11) Kilbourn, M. R.; Haka, M. S. Synthesis of [18F]GBR 13119 A Presynaptic Dopamine Uptake Antagonist. *Appl. Radiat. Isot*. **1988**, *39*, 279−282.

(12) Kilbourn, M. R. In Vivo Binding of [18F]GBR 13119 to the Brain Dopamine Uptake System. *Life Sci*. **1988**, *42*, 1347−1353.

(13) Kilbourn, M. R.; Carey, J. E.; Koeppe, R. A.; Haka, M. S.; Hutchins, G. A.; Sherman, P. S.; Kuhl, D. E. Biodistribution, Dosimetry, Metabolism and Monkey PET Studies of [18F]GBR 13119. Imaging the Dopamine Uptake System In Vivo. *Nucl. Med. Biol*. **1989**, *16*, 569−576.

(14) Fowler, J. S.; Volkow, N. D.; Wolf, A. P.; Dewey, S. L.; Schlyer, D. J.; Macgregor, R. R.; Hitzemann, R.; Logan, J.; Bendriem, B.; Gatley, S. J. Mapping Cocaine Binding Sites in Human and Baboon Brain In Vivo. *Synapse* **1989**, *4*, 371−377.

(15) Logan, J.; Fowler, J. S.; Volkow, N. D.; Wolf, A. P.; Dewey, S. L.; Schlyer, D. J.; Macgregor, R. R.; Hitzemann, R.; Bendriem, B.; Gatley, S. J.; Christman, D. R. Graphical Analysis of Reversible Radioligand Binding from Tome-Activity Measurements Applied to [N-11C-Methyl]-(−)-Cocaine PET Studies in Human Subjects. *J. Cereb. Blood Flow Metab*. **1990**, *5*, 740−747.

(16) Ding, Y.; Fowler, J.; Volkow, N.; Logan, J.; Gatley, S.; Sugano, Y. Carbon-11-d-*threo*-Methylphenidate Binding to Dopamine Transporter in Baboon Brain. *J. Nucl. Med*. **1995**, *36*, 2298−2305.

(17) Carroll, F. I.; Lewin, A. H.; Boja, J. W.; Kuhar, M. J.; Cocaine Receptor: Biochemical Characterization and Structure−Activity Relationships of Cocaine Analogues at the Dopamine Transporter. *J. Med. Chem*. **1992**, *35*, 969−981.

(18) Frost, J. J.; Rosier, A. J.; Reich, S. G.; Smith, J. S.; Ehlers, M. D.; Snyder, S. H.; Ravert H. T.; Dannals R. F. Positron Emission Tomographic Imaging of the Dopamine Transporter with ^{11}C-WIN 35,428 Reveals Marked Declines in Mild Parkinson's Disease. A*nn. Neurol*. **1993**, *34*, 423−431.

(19) Meltzer, P. C.; Liang, A. Y.; Brownell, A. L.; Elmaleh D. R.; Madras B. K. Substituted 3-phenyltropane Analogues of Cocaine: Synthesis, Inhibition of Binding at Cocaine Recognition Sites, and Positron Emission Tomography Imaging. *J. Med. Chem*. **1993**, *36*, 855−862.

(20) Dannals, R. F.; Neumeyer, J. L.; Milius, R. A.; Ravert, H. T.; Wilson, A. A.; Wagner, H. N., Jr. Synthesis of a Radiotracer for Studying Dopamine Uptake Site In Vivo Using PET: 2β-carbomethoxy-3β-(p-fluorophenyl)-[N-^{11}C-methyl]tropane ([^{11}C]-CFT or (^{11}C-WIN 35,428). *J. Lab. Comp. Radiopharm*. **1993**, *33*, 147−152.

(21) Brownell, A. L.; Elmaleh, D. R.; Meltzer, P. C.; Shoup, T. M.; Brownell, G. L.; Fischman A. J.; Madras B. K. Cocaine Congeners as PET Imaging Probes for Dopamine Terminals. *J. Nucl. Med*. **1996**, *37*, 1186−1192.

(22) Muller, L.; Halldin C.; Farde, L.; Karlson, P.; Hall, H.; Swahn, C. G.; Neumeyer, J. L.; Wang, S.; Milius, R. A. [^{11}C]β-CIT, a Cocaine Analogue: Preparation, Autoradiography and Preliminary PET Investigations. *Nucl. Med. Biol*. **1993**, *20*, 249−255.

(23) Brown, D. J.; Luthra, S. K.; Brown, G. D.; Carrol. F. I.; Kuhar, M. J.; Osman, S.; Waters, S. L.; Brady, F. [11C]RTI-121A Potential Radioligand For PET Studies of the Dopamine Transporter. *J. Lab. Comp. Radiopharm*. **1994**, *35*, 483.

(24) Lundkvist, C.; Halldin C.; Swahn, C. G.; Hall, H.; Karlson, P.; Nakashima, Y.; Wang, S.; Milius, R. A.; Neumeyer, J. L.; Farde, L. [O-Methyl-^{11}C]β-CIT-FP, a Potential Radioligand for Quantitation of the Dopamine Transporter: Preparation, Autoradiography, Metabolite Studies, and Positron Emission Tomography Examinations. *Nucl. Med. Biol*. **1995**, *22*, 905−913.

(25) Halldin, C.; Farde, L.; Lundkvist, C.; Ginovart, N.; Nakashima, Y.; Karlsson, P.; Swahn, C. G. [^{11}C]β-CIT-FE, a Radioligand for Quantitation of the Dopamine Transporter in the Living Brain Using Positron Emission Tomography. *Synapse* **1996**, *22*, 386−390.

(26) Chaly, T.; Dhawan, V.; Kazumata, K.; Antonini, A.; Margoulef, C.; Dahl, R.; Belakhef, A.; Margoulef, D.; Yee, A.; Wang, S.; Tamagnan, G.; Neumeyer, J. L.; Eidelberg D. Radiosynthesis of [^{18}F]N-3-Fluoropropyl-2β-Carbomethoxy-3β-(4-Iodophenyl)Nortropane and the First Human Study with Positron Emission Tomography. *Nucl. Med. Biol*. **1996**, *23*, 999−1004.

(27) Wilson, A. A.; DaSilva, J. N.; Houle, S. In Vivo Evaluation of [^{11}C]- and [^{18}F]-Labeled Cocaine Analogues as Potential Dopamine Transporter Ligands for Positron Emission Tomography. *Nucl. Med. Biol*. **1996**, *23*, 141−146.

(28) Goodman, M. M.; Keil, R.; Shoup, T. M.; Eshima, D.; Eshima, L.; Kilts, C.; Votaw, J.; Camp, V. M.; Votaw, D.; Smith, E.; Kung, M. P.; Malveaux, E.; Watts, R.; Huerkamp, M.; Garcia, E.; Hoffman J. M. Fluorine-18 Labeled 2β-Carbomethoxy-3β-(4-Chlorophenyl)-8-(-3-Fluoropropyl)nortropane (FPCT): A PET Radiotracer for Imaging Dopamine Transporters. *J. Nucl. Med*. **1997**, *38*, 119−126.

(29) Carroll, F. I.; Abraham, P.; Lewin, A. H.; Parham, K.; Boja, J. W.; Kuhar, M. J. Isopropyl and Phenyl Esters of 3β-(4-Substitutedphenyl)tropan-2β-carboxylic Acids. Potent and Selective Compounds for the Dopamine Transporter. *J. Med. Chem.* **1992**, *35*, 2497−2500.

(30) Subramanian, T.; Bakay, R. A. E.; Emerich, D. F.; Hoffman, J. M.; Goodman, M. M.; Miller, G. W.; Levey, A. I.; Hubert, G. W.; Batchelor, S.; Winn, S. R.; Watts, R. L. Polymer Encapsulated PC-12 Cells Demonstrate High Affinity Uptake of Dopamine In Vitro and [F-18]-DOPA Uptake and Metabolism After Intracerebral Implantation in Nonhuman Primates. *Cell Transplant.* **1997**, *6*, 469−477.

JM9902234